

Analysis of Mixed Convection and Free Convection in a Reduced Solar Collector Using a Nanofluid as Heat Transfer Fluid

Soumia Baali Cherif¹, Imene Rahmoune¹, Saadi Bougoul^{1,*}, and Ali J. Chamkha²

¹Department of Physics, Faculty of Matter Sciences, Applied Energetic Physics Laboratory (LPEA), University of Batna 1, 05000, Batna, Algeria

²Faculty of Engineering, Kuwait College of Science and Technology, Doha District, 35004, Kuwait

A three-dimensional investigation of mixed convection which occurs from Al_2O_3 -water nanofluid flow in tube of a reduced solar collector and free convection in air gap situated between cover of solar collector and its absorber was investigated. Heat transmission by conduction in absorber and cover as well as thermal losses to exterior expressed in form of a convective flux have also been taken into account. The different transport equations were solved using CFD-Fluent software which is founded on finite volume method and Boussinesq's law was introduced to take into account of buoyancy effects. In this investigation, thermal efficiency of solar collector was evaluated and use of nanofluids allows to increase this parameter which is generally low for this kind of thermal systems. Length of thermal regime established in the tube is proposed and this investigation is extended relative to other works developed in this research field. Results obtained gave an idea about the flow structure of the fluid under consideration in a tube of a solar collector and heat transmission mechanisms in air gap and in other elements of the solar collector. These results can facilitate design of this thermal system.

KEYWORDS: Solar Collector, Convection, CFD, Nanofluid.

1. INTRODUCTION

Today, particular attention has been given to the solar energy which represents a large part of renewable energies and which constitute a source of clean, free and inexhaustible energy. It can replace fossil energies which are a source of environmental pollution and production of greenhouse gases. In use of solar energy, it is useful to capture it and transform it into useful energy by using efficient conversion systems.

Among these systems, we find solar collectors and currently a great effort is being made to improve the efficiency of these thermal systems. To increase their efficiency, techniques consist in increasing heat transmission surface between the absorber and working fluid in a reduced volume and others are based on the choice of materials of the various components of these systems without making it very expensive. Currently, new complementary technology is being developed to make solar collectors more efficient, it consists of replacing the conventional heat transfer fluid (water, ...) by another having high thermal properties.

To make thermal properties of working fluid better, a procedure consists of suspending solid particles of materials considered as good conductors of heat in conventional fluids. Resulting fluid is called nanofluid.

Choi¹ developed the first experiment which consists in studying the suspension of small particles (nanometric) and detected a clear enhancement in thermal conductivity of obtained fluid relative to that of basic one, then several investigations were developed to understand structure and behavior of this category of fluids and to determine their physical properties. Maxwell² showed that thermal conductivity of classic fluid improves by introducing material particles of different shapes at different volume fractions.

Other studies have been directed by Eastman et al.³ and Choi et al.⁴ these authors noticed that thermal conductivity of nanofluids is important relative to that of conventional fluid. Concentration of nanofluids plays a very important role in improvement of heat transfer because its increase makes it possible to increase the corresponding thermal conductivity. However, by exceeding a certain value, the viscosity increases considerably and consequently the pressure drops become very significant, so an optimal value must be chosen.

In other studies, improvement of heat transfer has been investigated by suspending carbon nanotubes (CNT) and

*Author to whom correspondence should be addressed.

Email: saadi.bougoul@univ-batna.dz

Received: 8 September 2022

Accepted: 7 November 2022

grapheme in base fluid and results obtained shows that thermal conductivity of resulting fluid is high.⁵ Pandey and Nema⁶ have experimentally analyzed impact of Al_2O_3 -water nanofluid on heat transmission, wall friction and heat lost to outside in a counterflow heat exchanger. They obtained that thermal conductivity improves by 11% in this nanofluid having a volume fraction of 2%. To complete experimental analyses, a large number of numerical investigations were developed to determine impact of nanofluids on improvement of heat transmission resulting from different flows in various thermal installations.

To calculate thermal efficiency of a solar collector, study of heat transfer is essential and we distinguish three modes: conduction, thermal radiation and convection. Study of convection is essential in solar thermal technology.

To rise heat transfer, use of nanofluids is essential and several types of these fluids have been tested to study experimentally enhancement of heat transmission. Among these fluids, we find CuO-water, TiO_2 -water and Al_2O_3 -water which are the most manufactured and marketed. Studies of free, forced and mixed convection in cavities of square, rectangular, circular, trapezoidal shapes as well as other shapes L, C, H have been developed in an extensive way⁷⁻¹³ in the case where the considered nanofluid is reactive or not and with or without magnetohydrodynamics.

Other works are developed and we can cite that of Jakeer et al.¹⁴ which analyzed the nanofluid flow resulting from the mixed convection in an enclosure saturated with Darcian porous medium. Impact of MHD on a nanofluid flow resulting from free convection in a cavity having an inclination has been examined by Mansour et al.¹⁵ They noticed that magnetohydrodynamics modifies streamlines, isotherms, and average Nusselt number and significantly influences flow structure.

Galerkin finite element investigation of thermal behavior of Fe_3O_4 -MWCNT/water hybrid nanofluid introduced into a corrugated enclosure subject to a uniform magnetic field was developed by Mourad et al.¹⁶ It is showed that average Nusselt growths with Rayleigh number and porosity ratio and it presents a decrease with Hartmann number.

Further investigations were carried out in channels with different shapes of the cross section^{17,18} which they can be applied in different thermal installations such as design of electronic components, heat exchangers and solar collectors.

Solar collectors intervene in several applications, they are used as heating, desalination and drying systems and in particular in production of hot water. Several types of solar collectors are marketed and different investigations have been developed to know thermal behavior of these thermal systems. Mintsu et al.¹⁹ developed an optimization study of a solar collector made of a polymer material, this study is supplemented by a parametric study by looking at the variation effect of several parameters (length, mass flow,

air layer thickness, etc...) on solar collector thermal performance. Yousefi et al.²⁰ investigated empirically impact of the nanofluid chosen on a flat solar collector efficiency, they observed that growing volume fraction from 0.2 to 0.4% rises considerably this factor. Javadi et al.²¹ directed an investigation on enhancement of a solar collector performance by varying types of nanofluids, they observed that thermal conductivity of considered fluids affects significantly this parameter.

Studies conducted in this research area illustrate that application of nanofluids increases heat transmission and therefore solar collectors' performance.

Following investigations presented by various authors, motivation of this work comes to complete what has been done in this research field by analyzing mixed convection of Al_2O_3 nanofluid in a tube and free convection in air gap of a reduced solar collector. This seems useful and this analysis facilitates design and optimization of flat solar collectors.

In this work, we present more information about flow behavior of the considered nanofluid and modes of heat transmission in a solar collector by looking at the impact of Reynolds numbers and concentrations of Al_2O_3 -water on temperature variation, Nusselt number and thermal performance of the solar collector.

2. PHYSICAL MODEL

Figure 1(a) shows geometry to be considered which consists of a circular tube where heat transfer fluid circulates and a cover under which there is a small air layer. This tube is in perfect contact with absorber. These components constitute the studied solar collector.

Dimensions of studied solar collector are given in Figure 1(a). The choice of these dimensions is due to similar studies carried out in this field²² and which resemble to our work.

Cover and absorber thicknesses are 4 mm and 1 mm respectively.

In this analysis, heat transfer modes are evaluated in three areas of the solar collector:

- Mixed convection in tube (zone 1),
- Free convection in air gap (zone 2),
- Conduction in absorber and cover (zone 3).

In first zone, heat transfer and flow of used nanofluid due to three-dimensional mixed convection inside the tube are examined using the monophasic approach. Chosen nanoparticles volume fraction are 3% and 5% respectively. Flow of working fluid is considered laminar and stationary and the imposed Reynolds number varies between 40 and 200.

Nanofluid flow structure and heat transmission that occur in solar collector tube are studied by classical conservation laws taking into account various simplifying assumptions. Physical characteristics of this used fluid are considered invariant with temperature except density,

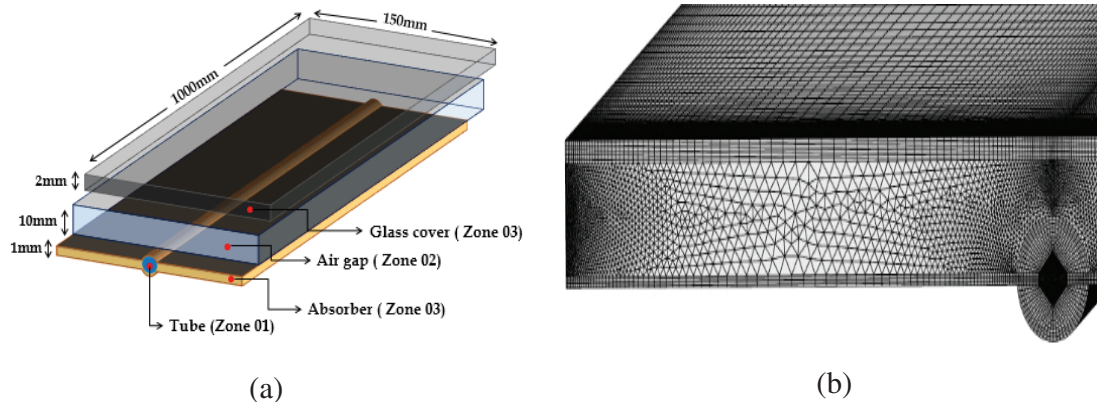


Fig. 1. Studied solar collector (a) and mesh of the computational domain (b).

which presents a variation taken into account into buoyancy forces. Considered fluid used in this analysis is considered to be incompressible and Newtonian and effects of thermal radiation is considered negligible.

In second zone, free convection takes place in the region located between cover and absorber which is filled with air. Studied flow is stationary and laminar and Boussinesq approximation is introduced to associate buoyancy effects. Physical phenomenon that occurs in this enclosure is partially similar to that of Rayleigh-Benard.

Heat transfer by conduction is studied in third part consisting of absorber and cover.

2.1. Mathematical Formulation

In following, three-dimensional and stationary equations of physical problem to be studied are presented. These equations give a study of flows resulting from mixed convection in tube and free convection in enclosure filled with air and placed between absorber and cover.

- Continuity:

$$\frac{\partial u}{\partial x} + \frac{\partial v}{\partial y} + \frac{\partial w}{\partial z} = 0 \quad (1)$$

- Momentum equation:

$$u \frac{\partial u}{\partial x} + v \frac{\partial u}{\partial y} + w \frac{\partial u}{\partial z} = -\frac{1}{\rho_{nf}} \frac{\partial P}{\partial x} + \nu_{nf} \left(\frac{\partial^2 u}{\partial x^2} + \frac{\partial^2 u}{\partial y^2} + \frac{\partial^2 u}{\partial z^2} \right) \quad (2)$$

$$u \frac{\partial v}{\partial x} + v \frac{\partial v}{\partial y} + w \frac{\partial v}{\partial z} = -\frac{1}{\rho_{nf}} \frac{\partial p}{\partial y} + \nu_{nf} \left(\frac{\partial^2 v}{\partial x^2} + \frac{\partial^2 v}{\partial y^2} + \frac{\partial^2 v}{\partial z^2} \right) + (\rho\beta)_{nf} g (T - T_0) \quad (3)$$

$$u \frac{\partial w}{\partial x} + v \frac{\partial w}{\partial y} + w \frac{\partial w}{\partial z} = -\frac{1}{\rho_{nf}} \frac{\partial P}{\partial z} + \nu_{nf} \left(\frac{\partial^2 w}{\partial x^2} + \frac{\partial^2 w}{\partial y^2} + \frac{\partial^2 w}{\partial z^2} \right) \quad (4)$$

- Energy equation:

$$u \frac{\partial T}{\partial x} + v \frac{\partial T}{\partial y} + w \frac{\partial T}{\partial z} = \alpha_{nf} \left(\frac{\partial^2 T}{\partial x^2} + \frac{\partial^2 T}{\partial y^2} + \frac{\partial^2 T}{\partial z^2} \right) \quad (5)$$

For nanofluid flow in absorber tube, we consider that solid particles are in thermal equilibrium with conventional fluid. Taking into account of Boussinesq's approximation, density variation with temperature is expressed as:

$$\rho = \rho_0 [1 - \beta(T - T_0)] \quad (6)$$

ρ_0 is the reference density at temperature T_0 and β is the thermal expansion coefficient at constant pressure.

Different laws used to determine physical characteristics of the fluid flowing through the tube are presented in the research work directed by Rahmoune et al.²³ and they are introduced into transport equations to determine the desired variables.

Average Nusselt number is calculated from this equation:²⁴

$$Nu_{nf} = h_{nf} D_h / K_f \quad (7)$$

h_{nf} is convective exchange coefficient and D_h is hydraulic diameter.

In the air gap, the same equations written before are used, it suffices to replace physical parameters of the nanofluid by those of air.

Dimensionless numbers Reynolds (Re), Grashof (Gr) and Richardson (Ri) involved in this study have the expressions:

$$Re = \frac{\rho_{nf} U_i D_h}{\mu_{nf}}, \quad Gr = \frac{g \beta_{nf} q_w D_h^4}{k_{nf} \nu_{nf}^2}, \quad Ri = \frac{Gr}{Re^2}$$

On the limits of the computational domain, these boundary conditions are imposed. At channel inlet, it is assumed that fluid has a uniform axial velocity U_i calculated from Reynolds number and a constant temperature T_o (300 K). At channel exit, outflow boundary condition is applied and for each wall, non-slip condition is imposed. In the middle

surface situated between two tubes, a condition of symmetry is applied.

A constant and uniform heat flow is imposed to the absorber plate which satisfies the following expression. It corresponds to the useful energy extracted by the collector under stationary conditions and it is related to the energy absorbed, less that lost by the collector to its environment. This can be summarized in the following equation:

$$Q = I(\alpha_1 \cdot \tau) - U_1(T_i - T_{amb}) \quad (8)$$

α , τ are absorption rate of the absorber and that of transmission of the cover I ($\text{W} \cdot \text{m}^{-2}$) represents solar radiation intensity. U is total heat transfer coefficient.

($\text{W} \cdot \text{m}^{-2} \cdot \text{K}^{-1}$) which represents inverse of all thermal resistances of solar collector.

The boundary conditions can be summarized:

- Tube inlet:

$$u = v = 0, \quad w = U_i, \quad T = T_o$$

- Absorber's upper surface

$$u = v = w = 0$$

$$Q = I(\alpha_1 \tau) - U_1(T_i - T_{amb}) = Cte$$

- Tube outlet:

$$\frac{\partial u}{\partial z} = \frac{\partial v}{\partial z} = \frac{\partial w}{\partial z} = 0$$

$$\frac{\partial T}{\partial z} = 0$$

At the solid-fluid interface:

$$k_f \left(\frac{\partial T}{\partial N} \right)_{\text{fluid}} = k_a \left(\frac{\partial T}{\partial N} \right)_{\text{solid}}$$

Where N is the distance along x or y or z .

3. NUMERICAL APPROACH

After meshing of the computational domain, Fluent-CFD software is used to resolve different equations associated with the boundary conditions of the problem to be solved. These partial differential equations are nonlinear. The numerical method used is that of finite volumes. Convective and diffusive terms of transport equations are approximated using a second-order UPWIND method. Semi Implicit Method for Pressure Linked Equations (SIMPLE) algorithm in monophasic approach is introduced to ensure pressure and velocity coupling. This method was investigated by Patankar.²⁵ As the different equations written before are coupled and nonlinear, they are solved by an iterative scheme and stability of this scheme is satisfied by employing under-relaxation coefficients.

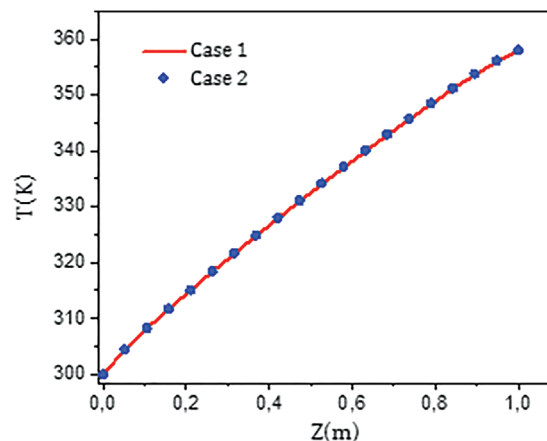


Fig. 2. Temperature variation along the tube axis for two different meshes.

Convergence was assured by values of imposed residuals as well as their variation. In numerical solution, adequate and imposed convergence criterion for all equations is 10^{-4} except for the energy equation where its value is taken equal to 10^{-6} .

The solution convergence is satisfied when the difference between two successive iterations for each variable is less than the imposed value of the residual. This is expressed by:

$$|\psi^{n+1} - \psi^n| \leq \varepsilon$$

ψ is the considered variable, n is the iteration number and ε the imposed residual.

The discretization of the studied volume was carried out using a non-uniform mesh.

As temperature and velocity variations are significant, a tight mesh in region near the inner walls of the tube was used. For the numerical method, it is important to control the mesh independence of the obtained results, this allows us to have correct results and to reduce calculation time. For two selected meshes (3171427, 5110335), temperature variation along the axis of the tube is represented in Figure 2. For our case, we opted for the first one.

For cover and absorber, number of nodes in the axial direction is the same as that of the tube. The cavity located between absorber and cover has been discretized by using a non-uniform mesh. Near walls, grid is refined to take into account of development of dynamic and thermal boundary layers (Fig. 1(b)).

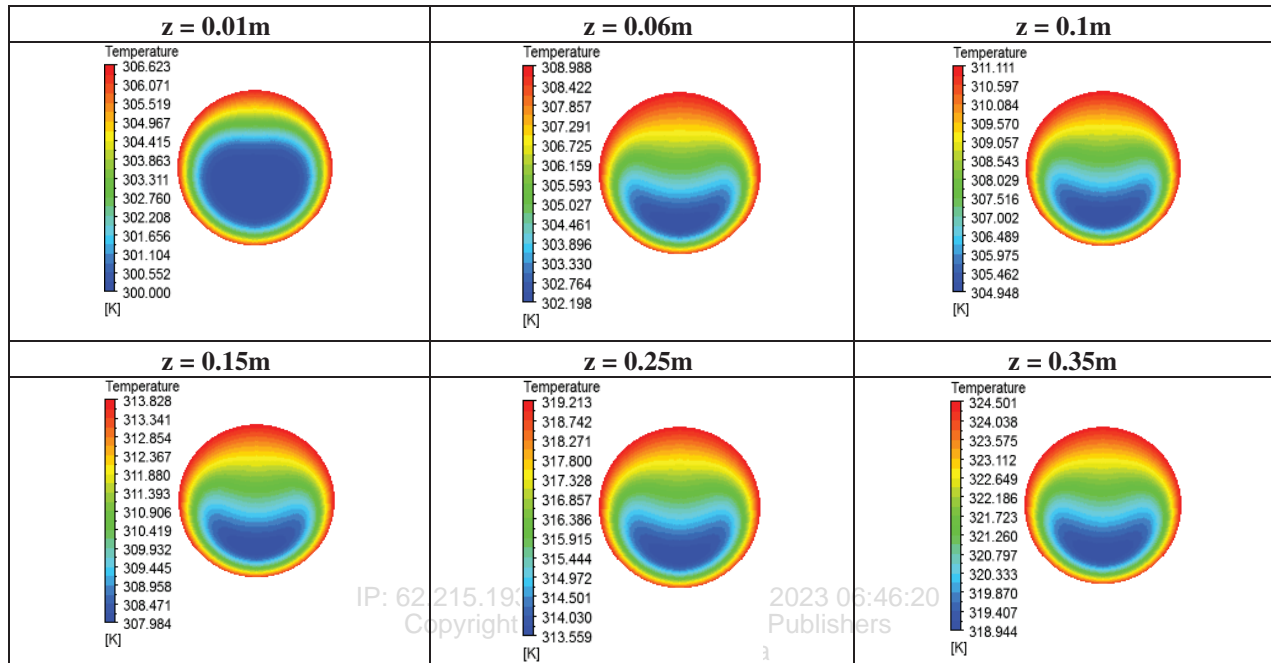
4. RESULTS AND DISCUSSION

Results of mixed convection in the tube, free convection in the air gap confined between absorber and cover and temperature variation in absorber and cover are presented. These results are compared with some results obtained by other authors.²²

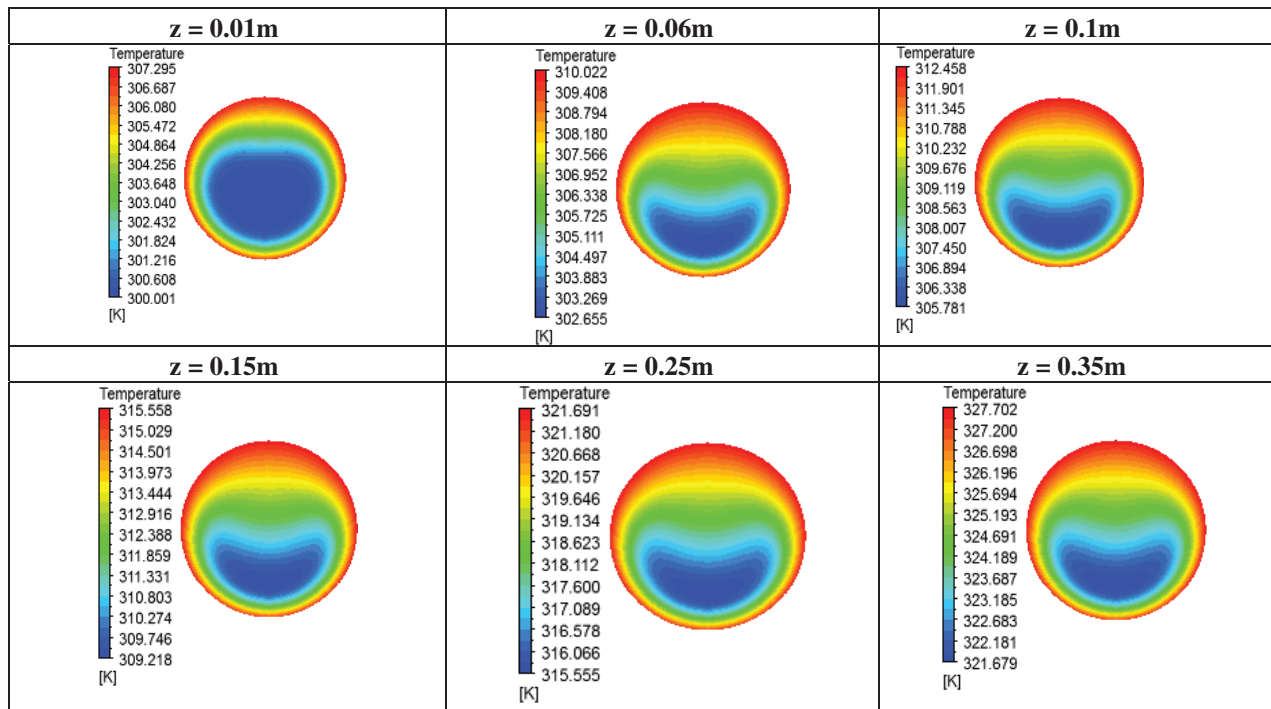
The simulations are conducted for two values of heating flux imposed on the absorber ($360 \text{ W}\cdot\text{m}^{-2}$ and $408 \text{ W}\cdot\text{m}^{-2}$) and for two volume fractions of the nanofluid (3% and 5%).

After several calculations and choices of the fluxes imposed on the absorber, these two values were chosen to

keep the study in the case of mixed convection controlled by Richardson number which must vary in the interval ($0.1 \leq Ri \leq 10$) for a fixed Grashof number and for a variable Reynolds number which takes the values 40, 80, 100 and 200.



(a)



(b)

Fig. 3. Temperature variation in various cross sections of tube for $Re=40$. (a) $\varphi=3\%$, (b) $\varphi=5\%$.

Heat flux fixed on absorber is equivalent to incident solar radiation and it corresponds to the boundary condition imposed on this surface.

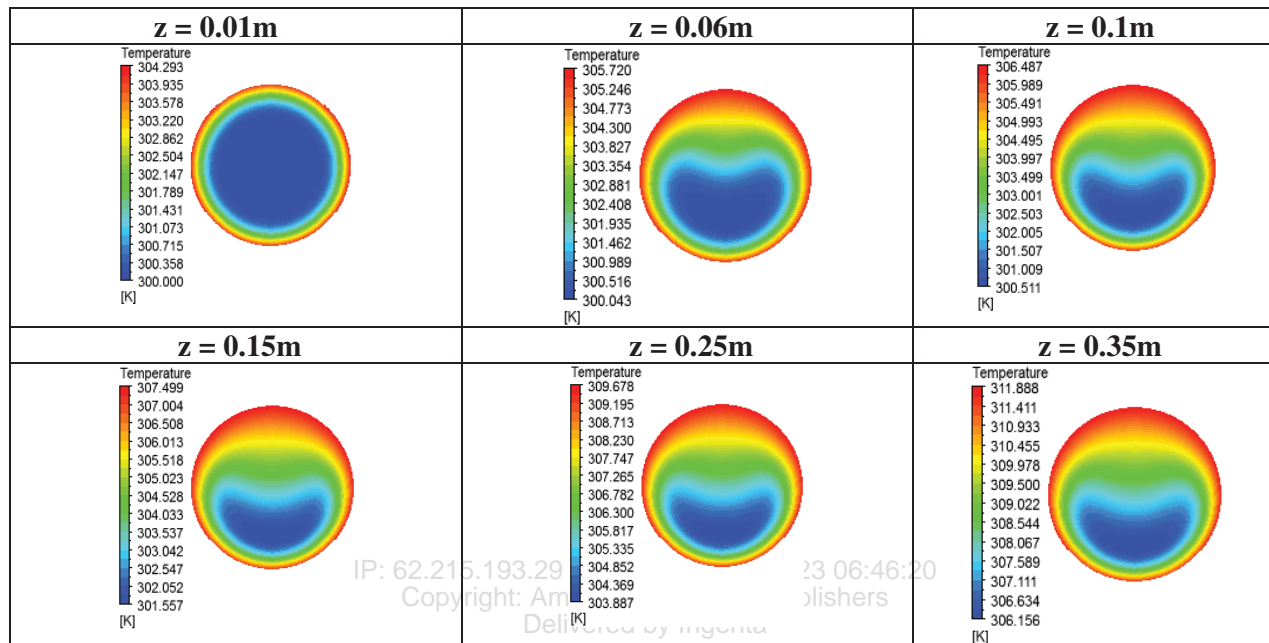
The ambient temperature is maintained equal to 293 K and the convective exchange coefficient imposed on the cover corresponds to the case where the wind speed is zero. This coefficient is calculated from the formula:²²

$$h = 5.7 + 3.8u_w, u_w \text{ is the wind velocity.}$$

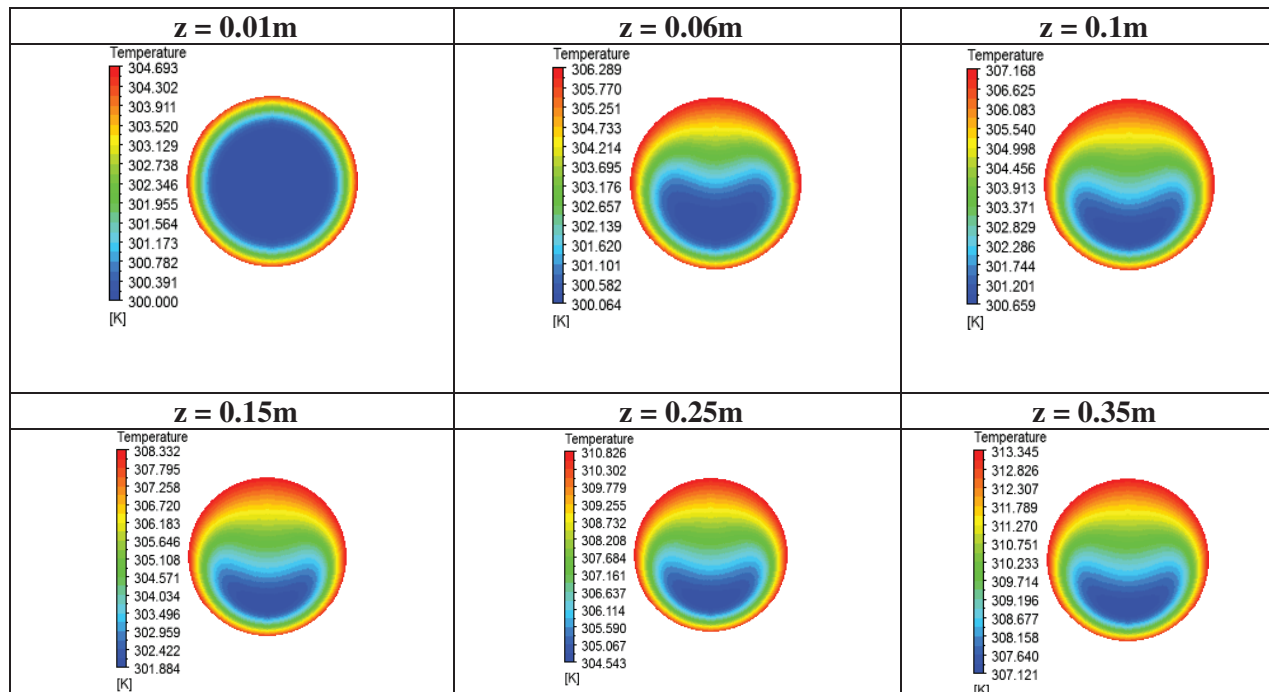
Other expressions can be used.²⁶

4.1. Study of Mixed Convection in the Tube

The velocity imposed at the inlet of the tube is calculated each time from the fixed values of the numbers of



(a)



(b)

Fig. 4. Temperature variation in various cross sections of tube for $Re = 100$. (a) $\phi = 3\%$, (b) $\phi = 5\%$.

Reynolds and Richardson and the temperature at the inlet is chosen equal to 300 K.

For a mass flow incoming tube and for heat flux applied to absorber, buoyancy effects occur. To measure the intensity of the mixed convection which results from the phenomena associated with natural convection and forced convection, we use the Richardson number which must be in the interval going from 0.1 to 10. In our case, the values chosen of Richardson varies between 0.2 and 5. In each cross-section, two convective cells occur and create secondary flow resulting from buoyancy effects. They raise the hot fluid along the wall and they lower it along the center of the tube. At inlet of tube, temperature distribution does not present a circumferential variation, therefore the wall-fluid exchange coefficient can be considered as uniform. In this case, boundary layer develops and buoyancy effects are not considerable and impact of natural convection are not significant.

Before reaching the established regime in a section perpendicular to the tube axis, it is noted that temperature variation is non-uniform and accumulation of hot fluid with a stratification occurs in the upper part of this section while the temperature remains almost constant at the bottom. This temperature variation is due to intense effects of secondary flows. This phenomenon is significant going along the length of the tube which favors the

development of the established regime. Then temperature variation becomes the same in two consecutive sections so mixed convection is established. Wall temperature depends on axial and tangential direction. Due to the asymmetry in the temperature profile in each cross section of tube, exchange coefficient between the wall and the fluid is not uniform.

According to results obtained, volume fractions does not influence the flow structure and the length where this flow develops (intersection of the two thermal boundary layers), and for high values of volume fractions, nanofluid temperature becomes high.

Reynolds number influences this length, when this number is high the length where the flow regime becomes fully developed becomes significant. Results obtained are represented in Figures 3–5.

Heat transmission between the absorber and the fluid flowing in the tube is related to the convective heat transfer coefficient which has a decreasing value according to the direction of the flow to reach a constant value once the thermal regime is established. For this, we propose an expression of the establishment length while keeping the same equation given in several Refs. [19, 27]

Following results obtained, we can propose an approximate thermal entry length which resembles that which

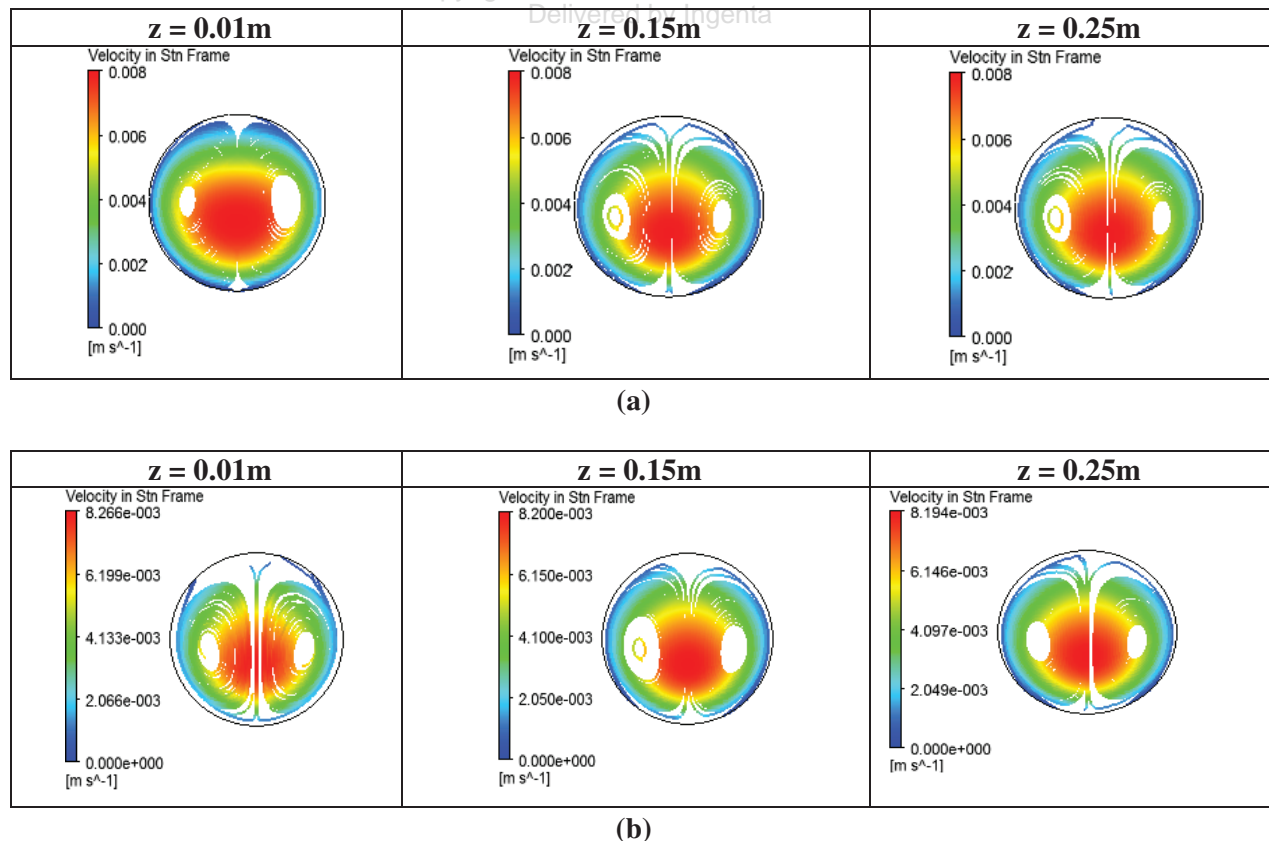


Fig. 5. Streamlines in different cross sections of tube for $Re=40$. (a) $\phi=3\%$, (b) $\phi=5\%$.

exists in theory for laminar flows. This length has the expression:

$$L_{t,laminar} = Cst \cdot Re \cdot D \cdot Pr \quad (9)$$

For each Reynolds number (Re), constant value is given. In this case, the Prandtl number (Pr) is less than 5, 6. D is hydraulic diameter. Constant has a value of 0.029 for Reynolds numbers equal to 40 and 100 and $\varphi=3\%$ and a value of 0.0316 for the same Reynolds numbers and $\varphi=5\%$. These constants are not far from those proposed by Cengel.²⁷

Nusselt number is determined by Eq. (7). Along tube wall, this number is presented in Figure 6. we noted that this number grows with volume fraction and Reynolds number. For Reynolds number values below 100, variation in Nusselt number with volume fraction is not too significant.

Outlet temperature decreases when Reynolds number (hence mass flow) increases. Increase in mass flow decreases heat transmission and fluid flowing through tube collects less heat from absorber. Nanofluid having high

volume fraction gives a high outlet temperature. This is shown in Figure 7. This figure gives the temperature variation according to the horizontal diameter of the tube, this variation depends of the secondary flow which occurs vertically. We note that temperature rises when the volume fraction increases.

4.2. Temperature Variation in the Absorber and the Cover

In zone located at inlet of the tube, boundary layer develops having a low thickness which gives a maximum heat exchange. Looking at absorber temperature variation (Fig. 8(a)), we can note that effect of heat transfer fluid on this variable is remarkable over a large area. When fully developed regime is reached, effect of coolant on absorber temperature is limited to a small area.

Thermal losses to the outside of solar collector are proportional to absorber temperature, if absorber temperature is high, energy emitted to cover by absorber is considerable and moreover if thermal gradients between absorber

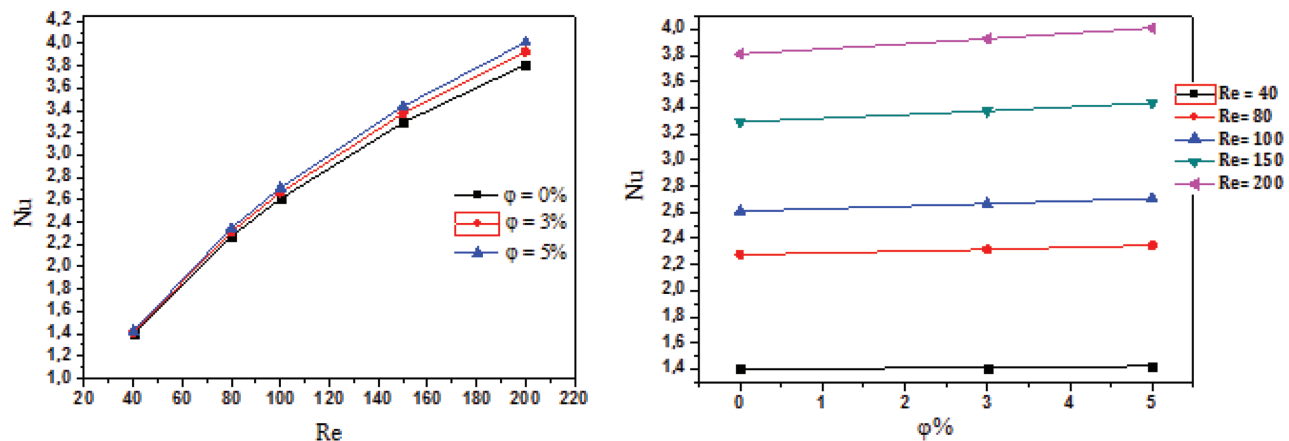


Fig. 6. Evolution of Nusselt number with Reynolds number and volume fraction.

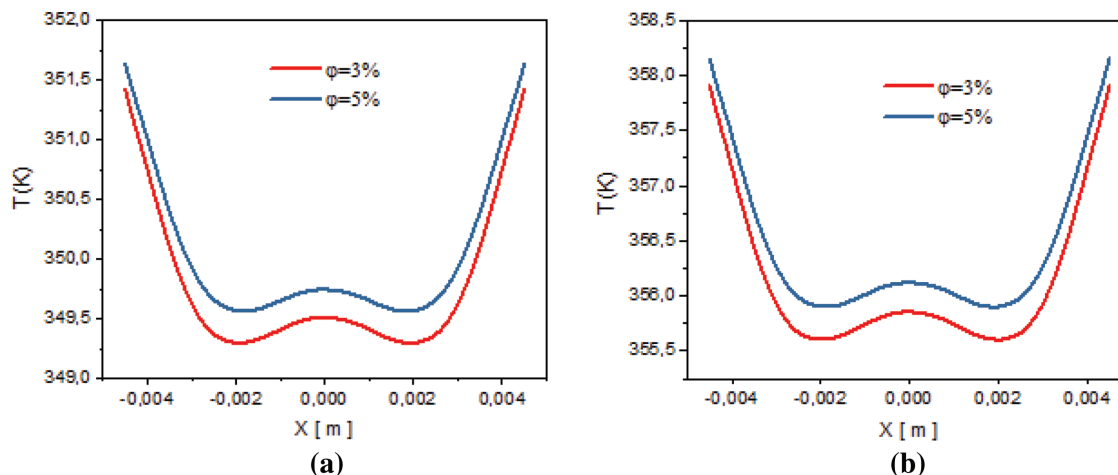


Fig. 7. Temperature variation in a tube section for $Re=40$ and for two values of the volume fraction. (a) First imposed heating flux, (b) second heating flux imposed.

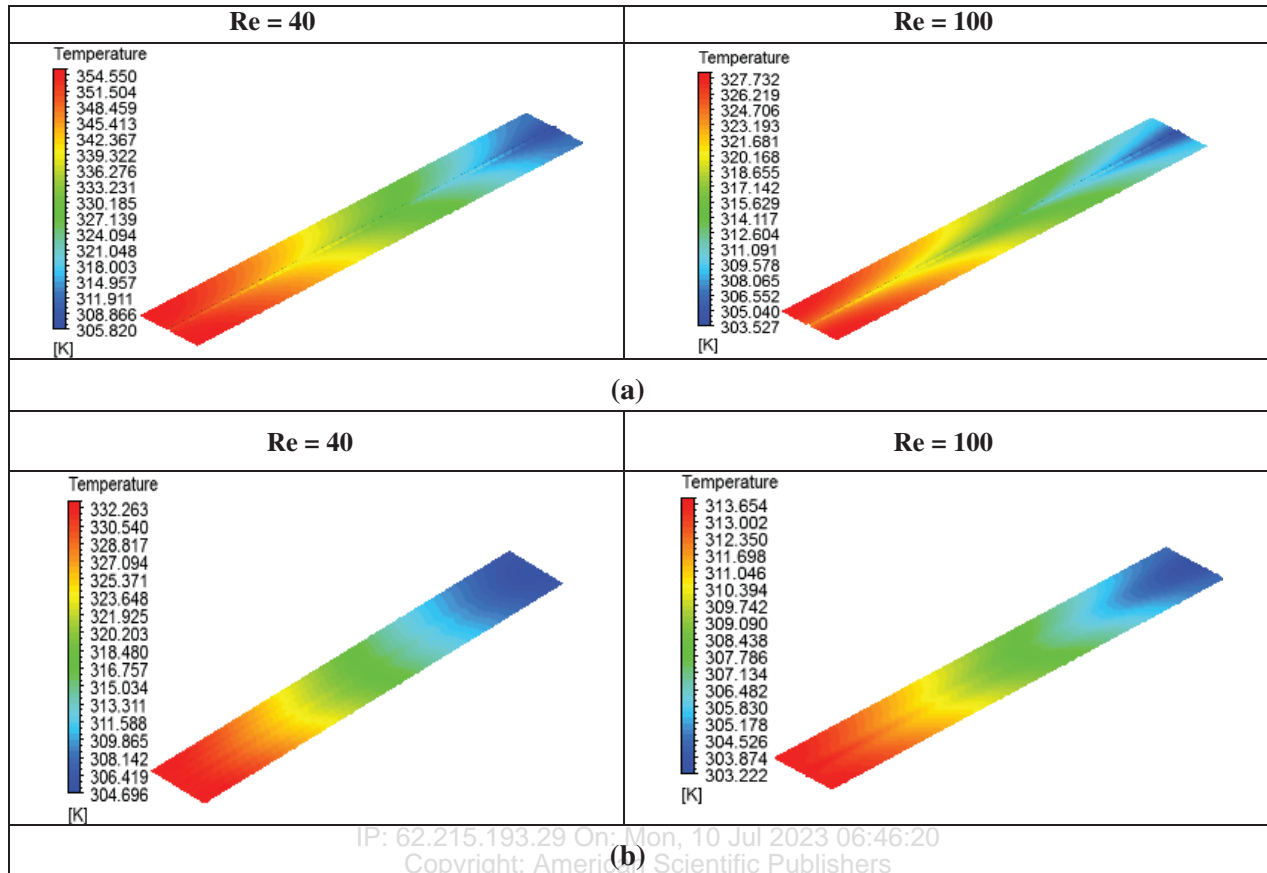


Fig. 8. Absorber (a) and cover (b) temperatures for $\varphi = 3\%$.

and cover are significant, heat transfer by free convection increases, which promotes heat losses to external environment. Absorber temperature influences heat losses, therefore, heat transmission between absorber and heat transfer fluid must be efficient. For temperature variation of the absorber, we can note that symmetry is well respected, this is represented in Figure 8(a).

Variation in cover temperature is given in Figure 8(b), we see that it is symmetrical and it follows the same variation as that of the absorber with a decrease in its values, therefore cover temperature is in close relationship with that of the absorber and consequently, it influences the convective transfer to outside. Heat transfer between absorber and cooling fluid is in a relationship with to the difference in their temperatures.

4.3. Free Convection in air gap

Thickness of air gap is chosen equal to 10 mm, this choice is due to the fact that analysis of performance of a solar collector has been carried out and maximum efficiency is obtained for the chosen thickness.¹⁹ For small thicknesses of air gap, conduction becomes dominant while convection becomes significant for great ones. Therefore, thickness of air gap must have an optimum to limit heat losses from absorber to outside.

For studies carried out, it has been found that despite thermal losses which remain low along cover for a thickness of air gap greater than 10 mm, efficiency of the solar collector decreases, this is due to natural convection which becomes intense in confined space and moving air carries energy from absorber and releases it to collector cover. Velocity variation in air gap is given in Figure 9.

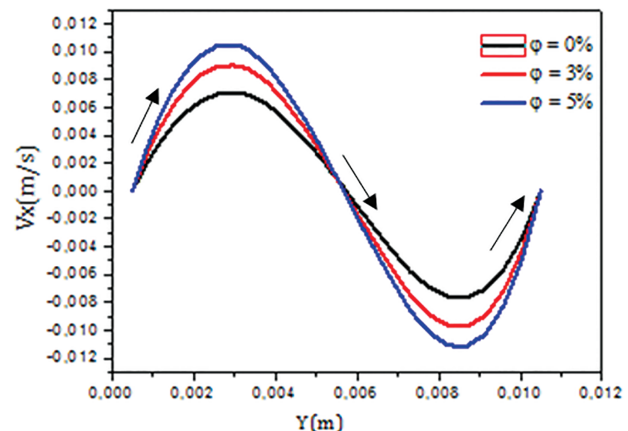


Fig. 9. Air velocity in air gap.

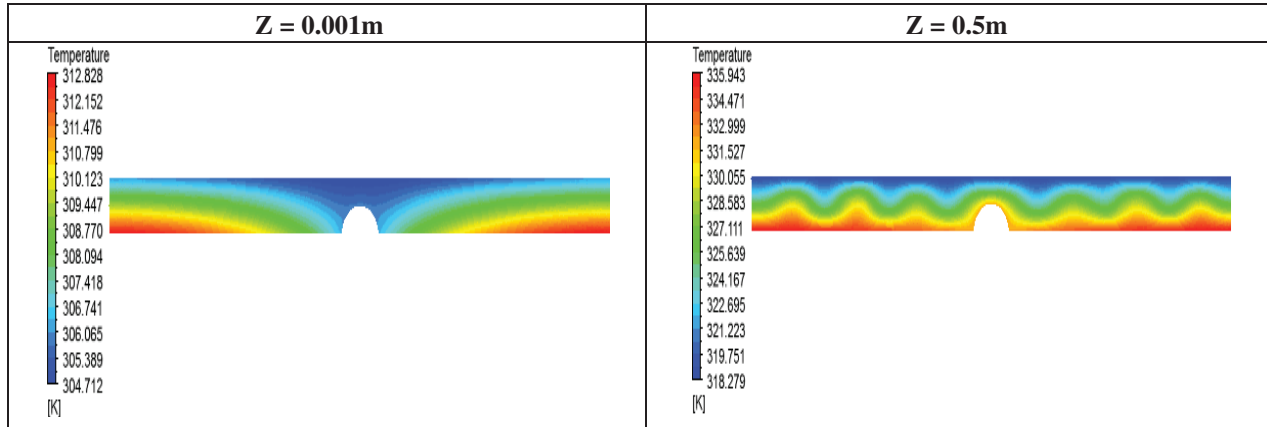


Fig. 10. Temperature variation in the air gap for two cross sections for $\phi = 3\%$ and $Re = 40$.

This curve highlights presence of free convection in confined space positioned between absorber and cover. Air circulation in this zone is due to buoyancy forces which are due to difference in densities. As we can see, air velocity increases along absorber (ordinate $Y = 0$) and decreases along collector cover ($Y = 10$ mm). We notice that for high volume fractions of nanofluid, fluid becomes accelerated (see Fig. 9), this is related to the volume fraction which has an impact on the streamlines. Temperature variation for study of free convection in air gap is shown in Figure 10. This air gap is characterized by a large aspect factor.

As it can be shown in this figure, absorber temperature is not uniform, so in certain sections of air gap positioned near the inlet zone of cooling fluid, heat transfer takes place by conduction (diffusion) and in other sections further from the inlet where temperature gradient between absorber and cover is important, heat transmission by free convection occurs and gives rise to a multicellular flow equivalent to that of Rayleigh-Benard. The inhomogeneous absorber temperature field results in an irregular variation of cells in successive cross-sections. This is evidenced by study of Cerón et al.²²

The multicellular flow is noted in the case of low Reynolds numbers because temperature difference between absorber and cover in some sections is important which favors air movement by natural convection contrary to the case of high Reynolds numbers where conduction becomes dominant and heat transfer occurs by diffusion.

4.4. Solar Collector Performance

In this part, we proceed to evaluation of the solar collector performance.

Thermal efficiency of the solar collector can be expressed as the ratio of useful power supplied and heating flux applied to the absorber. This is given by the following expression:

$$\eta = \frac{Q}{A_{ab}I} \tag{10}$$

The useful heat Q represents the useful heat collected which is given by:

$$Q = mc_p(T_o - T_i) \tag{11}$$

Where m is mass flow, c_p is specific heat at constant pressure and $T_o - T_i$ is the difference between outlet and inlet temperatures of used fluid. For chosen values of volume fractions, thermal efficiency of solar collectors rises, this is due to improvement in nanofluid thermal conductivity.

In figure below (Fig. 11), we give variation of thermal efficiency of the solar collector according to Reynolds number, we also note that the thermal performance increases for the chosen values of Reynolds and it is better for the case of nanofluid than for the case of conventional fluid.

For the second heat flux imposed on the absorber, for a volume fraction of 5% and a Reynolds number equal to 40, we show three-dimensional variation of the temperature

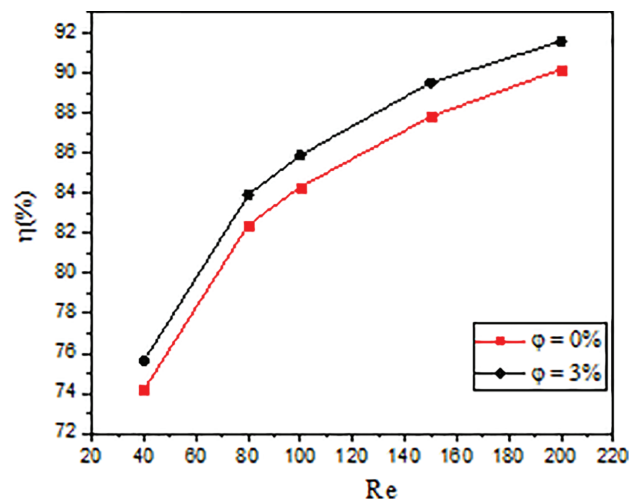


Fig. 11. Thermal performance variation of the solar collector with Reynolds number.

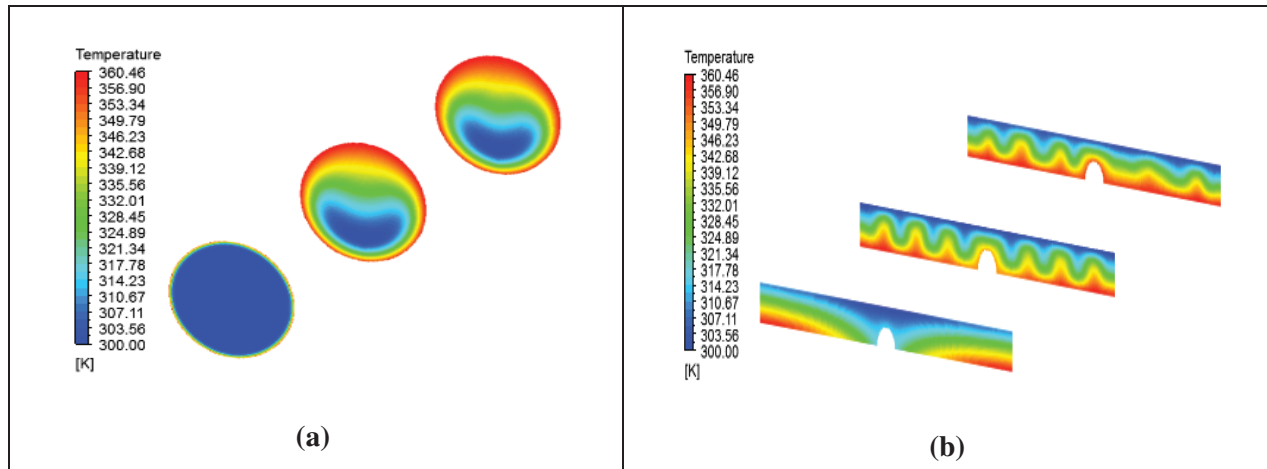


Fig. 12. Three-dimensional temperature variation. (a) In the tube; (b) In the air gap.

of the nanofluid in the tube and in the air gap, this gives an idea of the thermal behavior of the nanofluid flowing through the tube and of heat transmission that occurs in air gap. Figure 12 gives this temperature variation.

5. CONCLUSION

A numerical model for a flat solar collector consisting of a tube in perfect contact with an absorber surmounted by an air gap confined between absorber and cover has been developed. In this study, we have developed a detailed analysis of mechanisms of heat transmission in various components of solar collector under the boundary conditions imposed. Temperature field in absorber and in cover was determined and the flow structure and thermal behavior of nanofluid in the tube were investigated. This analysis is supplemented by study of free convection in air gap.

The main conclusions drawn are:

- Examination of mixed convective heat transmission inside the tube revealed a higher Nusselt number with increasing nanofluid volume fraction. Buoyancy effects associated with main flow of nanofluid favor a rise in heat transfer rate.
- Study of free convection in air gap shows that in region which corresponds to the entry of the coolant and for high Reynolds numbers, heat transfer is generally done by conduction, however for low Reynolds numbers and moving away from fluid inlet region, we see the appearance of convection cells and due to non-uniform temperature of absorber these cells are formed in a discontinuous way along the air gap. These cells sometimes promote heat loss to the outside by heating the glass of the solar collector what influences the thermal performance of the solar collector.

For chosen Reynolds numbers, Nusselt number increases and consequently heat transfer coefficient increases which improves the energy system efficiency.

- A correlation of the length of the fully developed thermal regime in the tube has been proposed and this correlation is not very different from those given by classical laws.

- Until 5% of the nanofluid volume fraction (maximum value chosen in this study), presence of nanoparticles in heat transfer fluid gives an improvement in thermal performance of the solar collector.

NOMENCLATURE

- A absorber area [m^2]
- c_p specific heat at constant pressure [$\text{J} \cdot \text{Kg}^{-1} \cdot \text{K}^{-1}$]
- D_h Hydraulic diameter [m]
- g gravitational acceleration [$\text{m} \cdot \text{s}^{-2}$]
- h convection heat transfer coefficient [$\text{W} \cdot \text{m}^{-2} \cdot \text{K}^{-1}$]
- I intensity of the solar radiation [$\text{W} \cdot \text{m}^{-2}$]
- L_t thermal entry length [m]
- \dot{m} mass flow [$\text{Kg} \cdot \text{s}$]
- P pressure [Pa]
- q_w heat flux [$\text{W} \cdot \text{s}^{-2}$]
- Q heat collected [$\text{W} \cdot \text{m}^{-2}$]
- T temperature [K]
- u, v, w velocity components [$\text{m} \cdot \text{s}^{-1}$]
- u_w wind velocity [$\text{m} \cdot \text{s}^{-1}$]
- U_1 overall heat transfer coefficient [$\text{W} \cdot \text{m}^{-2} \cdot \text{K}^{-1}$]
- x, y, z cartesian coordinates [m]

Greek Symbols

- α thermal diffusivity [$\text{m}^2 \cdot \text{s}^{-1}$]
- ρ density [$\text{Kg} \cdot \text{m}^{-3}$]
- β coefficient of thermal expansion [K^{-1}]
- η thermal performance [%]
- μ dynamic viscosity [$\text{Kg} \cdot \text{m}^{-1} \cdot \text{s}^{-1}$]
- ν kinematic viscosity [$\text{m}^2 \cdot \text{s}^{-1}$]
- φ Volume fraction [%]

Subscripts

- ab* absorber plate
amb ambient
avg average
f fluid
nf nanofluid
gc glass cover
s nanoparticle
i, o inlet and outlet

Dimensionless Numbers

- Gr* Grashof number
Nu Average Nusselt number
Re Reynolds number
Pr Prandtl number
Ri Richardson number
Ra Rayleigh number

Optical Parameters

- α_1 absorptivity
 τ transmissivity

References and Notes

- S. U. S. Choi, *ASME Journal of Heat Transfer*, ASME, 66, 99 (1995).
- J. C. Maxwell, *A Treatise on Electricity and Magnetism*, 2nd ed., Oxford University Press, Cambridge (1881).
- J. A. Eastman, S. U. S. Choi, S. Li, W. Yu, and L. J. Thompson, *Appl. Phys. Lett.* 78, 718 (2001).
- S. U. S. Choi, Z. G. Zhang, W. Yu, F. E. Lockwood, and E. A. Grulke, *Appl. Phys. Lett.* 79, 2252 (2001).
- R. Kamali and A. R. Binesh, *International Communications in Heat and Mass Transfer* 37, 1153 (2010).
- S. D. Pandey and V. K. Nema, *Exp. Therm. Fluid Sci.* 38, 248 (2012).
- R. Mohebbi and M. M. Rashidi, *Journal of the Taiwan Institute of Chemical Engineers* 72, 70 (2017).
- N. Makulati, A. Kasaeipoor, and M. M. Rashidi, *Adv. Powder Technol.* 27, 661 (2016).
- B. Ghasemi, *Numerical Heat Transfer, Part A: Applications* 63, 473 (2013).
- S. Hussain, S. E. Ahmed, and T. Akbar, *Int. J. Heat Mass Transfer* 114, 1054 (2017).
- M. H. Tilehnoee, A. S. Dogonchi, S. M. Seyyedi, A. J. Chamkha, and D. D. Ganji, *J. Therm. Anal. Calorim.* 141, 2033 (2020).
- I. Rahmoune, S. Bougoul, and A. Chamkha, *J. Nanofluids* 11, 1 (2022).
- S. Sivasankaran, M. A. Mansour, A. M. Rashed, and M. Bhuvaneshwari, *Numerical Heat Transfer; Part A* 70, 1356 (2016).
- S. Jakeer, P. BalaAnki Reddy, H. A. Rashad, and H. A. Nabwey, *Alexandria Engineering Journal* 60, 821 (2021).
- M. A. Mansour, G. R. Subba Reddy, S. Siddiqua, A. M. Rashed, and T. Salah, *International Journal of Nonlinear Sciences and Numerical Simulation* 000010151520200138 (2021).
- A. Mourad, A. Aissa, F. Mebarek-Oudina, W. Jamshed, W. Ahmed, H. M. Ali, and A. M. Rashad, *International Communications in Heat and Mass Transfer* 126, 105461 (2021).
- H. Demir, A. S. Dalkilic, N. A. Kurekci, W. Duangthongsuk, and S. Wongwise, *International Communications in Heat and Mass Transfer* 38, 218 (2011).
- I. Rahmoune and S. Bougoul, *Journal of Applied Mechanics and Technical Physics* 62, 920 (2021).
- A. C. Mints Do Ango, M. Medale, and C. Abid, *Solar Energy* 87, 64 (2013).
- T. Yousefi, F. Veysi, E. Shojaeizadeh, and S. Zinadini, *Exp. Therm. Fluid Sci.* 39, 207 (2012).
- F. S. Javadi, R. Saidur, and M. Kamalisarvestani, *Renewable and Sustainable Energy Reviews* 28, 232 (2013).
- J. F. Cerón, J. Pérez-García, J. P. Solano, A. García, and R. Herrero-Martin, *Applied Energy* 140, 275 (2015).
- I. Rahmoune, S. Bougoul, and A. J. Chamkha, *The European Physical Journal Special Topics* 231, 2901 (2022).
- M. M. Rahman, S. Mojumder, S. Saha, S. Mekhilef, and R. Saidur, *International Communications in Heat and Mass Transfer* 57, 79 (2014).
- S. V. Patankar, *Numerical Heat Transfer and Fluid Flow*, McGraw-Hill, Washington, New York (1980).
- S. Zeroual, S. Bougoul, and H. Benmoussa, *J. Appl. Mech. Tech. Phy.* 59, 1008 (2018).
- Y. A. Cengel, *Heat and Mass Transfer*, 3rd Ed., McGraw-Hill, New York (2007).